Conformational and Molecular Modeling Studies of β-Cyclodextrin−Heptagastrin and the Third Extracellular Loop of the Cholecystokinin 2 Receptor†

Craig Giragossian,‡ Norbert Schaschke,§ Luis Moroder,§ and Dale F. Mierke*,‡,||

Department of Chemistry and Department of Molecular Pharmacology, Division of Biology and Medicine, Brown University, Providence, Rhode Island 02912, and Max-Planck Institute of Biochemistry, 82152 Martinsried, Germany

Received August 22, 2003; Revised Manuscript Received January 14, 2004

ABSTRACT: The conformational features of a conjugate of the C-terminus of human gastrin (HG[11−17]), the shortest gastrin sequence retaining biological function, with β-cyclodextrin ([Nle^{15}]-HG[11−17]−βCD) were determined by NMR spectroscopy in an aqueous solution of dodecylphosphocholine (DPC) micelles. The peptide−βCD conjugate displays a binding affinity and activation profile comparable to those of HG[11−17] at the cholecysokinin 2 (CCK_2) receptor, the G protein-coupled receptor responsible for the gastrointestinal function of gastrin. The structure of the peptide consisted of a well-defined β-turn between Gly^{13} and Asp^{16} of gastrin. The structural preferences of [Nle^{15}]-HG[11−17]−βCD in DPC micelles and the 5-doxylstearate-induced relaxation of the ^{1}H NMR resonances support a membrane-associated receptor recognition mechanism. Addition of [Nle^{15}]-HG[11−17]−βCD to the third extracellular loop domain of the CCK_2 receptor, CCK_2-R(352−379), generated a number of intermolecular nuclear Overhauser enhancements (NOEs) and chemical shift perturbations. NOE-restrained MD simulations of the [Nle^{15}]-HG[11−17]−βCD−CCK_2-R complex produced a topological orientation in which the C-terminus was located in a shallow hydrophobic pocket near the confluence of TM2 and -3. Despite the steric bulk and physicochemical properties of βCD, the [Nle^{15}]-HG[11−17]−βCD−CCK_2-R complex is similar to the CCK-8−CCK_2-R complex determined previously, providing insight into the mode of ligand binding and the role of electrostatic interactions.

The cholecystokinin 2 (CCK_2)[1] guanine nucleotide-binding regulatory protein-coupled receptor (GPCR) is activated by cholecystokinin and gastrin, two endogenous peptides sharing an identical carboxyamidated C-terminal pentapeptide (Gly-Trp-Met-Asp-Phe-NH_2). Gastrin (HG) and cholecystokinin (CCK) are derived from distinct preprohormones and exist in multiple molecular forms (e.g., HG-34, HG-17, HG-7, CCK-33, CCK-8, and CCK-4); however, only the carboxyamidated C-terminal tetrapeptide is necessary for exerting the full biological effect (*1*, *2*). The CCK_2-R is expressed throughout the central nervous system (CNS), where it is involved in anxiety, satiety, analgesia, and memory (*2*, *3*). The receptor is also found in the gastrointestinal (GI) tract, where it regulates the proliferation of cells in the gastric mucosa, the contraction of smooth muscle cells in the stomach, and the secretion of gastric acid and pepsinogen (*2*, *3*). As such, the CCK_2-R has provided a potential therapeutic target for modulating neuronal and GI homeostasis (*4*).

The rational design of agonists and antagonists for the CCK_2-R, as for the vast majority of GPCRs, has been hindered by the lack of high-resolution structural data for the receptor and the ligand−receptor complexes. Therefore, structural studies have focused on delineating the conformational features of ligands in solvent systems that mimic the physicochemical environment of the ligand-binding pocket (*5*). Circular dichroism (CD) and NMR studies of cholecystokinin and gastrin in organic solvent/water mixtures were indicative of partially ordered structures composed of α helix, β form, and random coil (*6*−*11*). Structural studies of cholecystokinin in a membrane mimetic solvent system composed of dodecylphosphocholine (DPC) micelles revealed the preference for a pseudohelix in the C-terminal heptapeptide (*12*, *13*). Combined with the intermolecular contacts deduced by site-directed mutagenesis and photoaffinity cross-linking, the structural features of cholecystokinin and gastrin analogues have been used to define the ligand-binding pockets in molecular models of the ligand−receptor complexes (*14*−*18*).

Additional information concerning the ligand binding mechanism in the gastrin−CCK_2-R complex has been provided by N-terminal lipophilic and hydrophilic derivatives

† This work was supported, in part, by the National Institutes of Health (Grant GM 54082) and the American Heart Association, through an Established Investigator Award.

* To whom correspondence should be addressed: Department of Molecular Pharmacology, Division of Biology and Medicine, Brown University, Providence, RI 02912. Phone: (401) 863-2139. Fax: (401) 863-1595. E-mail: Dale_Mierke@Brown.edu.

‡ Department of Chemistry, Division of Biology and Medicine, Brown University.

§ Max-Planck Institute of Biochemistry.

|| Department of Molecular Pharmacology, Division of Biology and Medicine, Brown University.

[1] Abbreviations: βCD, β-cyclodextrin; CCK, cholecystokinin; CCK_1-R, cholecystokinin type 1 receptor; CCK_2-R, cholecystokinin type 2 receptor; DG, distance geometry; DPC, dodecylphosphocholine; EC, extracellular loop; G-protein, guanine nucleotide-binding regulatory protein; HG, human gastrin; MD, molecular dynamics; Nle, norleucine; NMR, nuclear magnetic resonance; NOE, nuclear Overhauser enhancement; NOESY, nuclear Overhauser enhancement spectroscopy; rmsd, root-mean-square deviation; TM, transmembrane; TOCSY, total correlation spectroscopy.

10.1021/bi035509w CCC: $27.50
Published on Web 02/19/2004

of gastrin (*17*, *19*). Dimyristoylated (DM) [Nle^{15}]-HG-17 and β-cyclodextrin conjugates of tetra- and heptagastrin exhibited a 4−7-fold reduction in receptor binding affinity in comparison to the unmodified peptides (*17*, *19*). The high affinity of DM-[Nle^{15}]-HG-17 is consistent with a membrane-associated pathway, whereby the ligand initially partitions into the cell membrane and then interacts with the receptor through a lateral diffusion process (*7*, *20*−*23*). However, the affinities of the β-cyclodextrin (βCD) conjugates suggest an alternative mechanism in which receptor recognition occurs by a more direct pathway via statistical collision in the aqueous phase (*19*). The interpretation of the binding results was further complicated by the inability to identify structural preferences for DM-[Nle^{15}]-HG-17 in either dimyristoylphosphatidylcholine (DMPC) vesicles or water (*7*).

Recently, X-ray crystallography and NMR spectroscopy have been used to determine the structure of receptor fragments corresponding to complete or partial domains of GPCRs, as well as the structure of the ligand−receptor domain complexes (*24*−*27*). The receptor domain approach has been used to deduce intermolecular contacts between CCK-8 and receptor domains derived from the human N-terminal (NT) domain of CCK$_1$-R(1−47) and the third extracellular loop domains of CCK$_1$-R(329−357) and CCK$_2$-R-(352−379) (*12*, *28*, *29*). The technique has since been extended to elucidate intermolecular contacts between synthetic agonists and CCK$_1$-R(329−357) (*30*). Incorporation of the experimentally determined structures and NOE-derived ligand−receptor contacts into molecular models of the full receptor produced binding orientations consistent with mutagenesis and photoinduced cross-linking studies (*13*, *28*, *29*).

In this study, the conformational features of the [Nle^{15}]-HG[11−17]−βCD conjugate were determined by NMR spectroscopy in a biphasic solvent system composed of an aqueous solution of DPC micelles. Addition of the ligands to the third extracellular loop of CCK$_2$-R(352−379) produced a number of intermolecular NOEs and ligand-induced chemical shift perturbations. The intermolecular NOEs were used to manually dock the [Nle^{15}]-HG[11−17]−βCD conjugate to an NOE-restrained molecular model of the CCK$_2$-R. The binding orientations and intermolecular interactions in the [Nle^{15}]-HG[11−17]−βCD−CCK$_2$-R complex are compared to those in the NOE-restrained molecular models of the CCK-8−CCK$_2$-R and CCK-8−CCK$_1$-R complexes.

EXPERIMENTAL PROCEDURES

Peptide Synthesis. A peptide corresponding to the putative EC3 domain and several residues from the adjoining sixth and seventh transmembrane (TM) domains of the human CCK$_2$-R, acetyl-A^{353}NTWRAFDGPGAHRALSGAPISFIH-LLS^{379}-NH$_2$, was synthesized using Fmoc chemistry (Protein Chemistry Facility, Tufts University, Boston, MA). The peptide was purified by semipreparative reverse-phase high-performance liquid chromatography, and the structural integrity was verified by mass spectrometry and NMR. The synthesis of the βCD conjugate of [Nle^{15}]-HG[11−17], AYGW(Nle)DF-NH$_2$, has been described previously (*19*). The preparation of CCK-8, DYMGWMDF-NH$_2$, has been described previously in detail (*28*).

NMR Methods. Peptide solutions (1 mM) were prepared in 50 mM phosphate buffer (90% H$_2$O/10% D$_2$O, Cambridge Isotopes) and 150 mM DPC-d_{38} (98.6%, Cambridge Isotopes). The pH of the solution was 5.2 without correcting for the deuterium isotope effect. Phase sensitive (*31*) TOCSY (*32*, *33*) and NOESY (*34*, *35*) spectra were collected using Bruker Avance 400 and 600 MHz NMR spectrometers (298−308 K, $f_2 = 2048$, $f_1 = 640$, 4−48 scans, SW = 7500 Hz) with mixing times of 50 and 150−300 ms, respectively. The WATERGATE pulse sequence was used for solvent suppression (*36*). The spectra were processed using NMRPipe (*37*). The NOE cross-peak volumes were integrated using Sparky (*38*) and converted to distances using the isolated two-spin approximation. The geminal cross-peak volumes of Asp^{16} and Phe^{17} were used as an internal reference (1.75 Å).[2] The upper distance restraints of nonstereospecifically assigned protons were corrected using standard procedures (*39*).

Studies of Radical-Induced Relaxation. The relative orientation of amino acid residues along the water−micelle interface was probed by monitoring radical-induced relaxation of the ^{1}H resonances (*40*). An aliquot of 5-doxylstearic acid dissolved in methanol was added, providing approximately one radical for each micelle of DPC.

Structure Calculations. The conformational space of the [Nle^{15}]-HG[11−17]−βCD conjugate was searched using distance geometry (DG) with random metrization (*41*). The experimentally derived distances, holonomic distances, and chiral volumes were used as restraints, generating an ensemble of 93 structures. A single structure, representative of the φ and ψ dihedral angle distributions of the entire ensemble and with small residual distance and chiral volume penalty functions, was selected for further refinement by NOE-restrained MD simulations (200 ps at 300 K). The peptide was placed in the center of a water/decane solvent box ($x = y = z = 60$ Å), with the side chains of Asp^{16} and Tyr^{12} and the βCD moiety projected into the aqueous phase. The side chain of Asp^{16} was treated as a charged species. The integration time step was 1 fs, and the neighbor list was updated every 10 fs. Lennard-Jones and Coulomb potentials were truncated with a polynomial switch function between 1.0 and 1.2 nm. Initial velocities were assigned randomly from a Maxwellian distribution and scaled to reflect the initial temperature of the system. The temperature was coupled with a time constant of 20 fs to an external bath using the method of Berendsen. A force constant of 2000 kJ mol^{-1} nm^{-2} was applied to the distance restraints throughout the entire simulation.

Models of the [Nle^{15}]-HG[11−17]−βCD−CCK$_2$-R(352−379) Complex. The previously reported structure of CCK$_2$-R-(352−379) (*29*) was template forced to the corresponding TM6 and -7 residues in the crystal structure of bovine rhodopsin (*42*). The template forcing resulted in a slight decrease in the minimum distance between TM domains (from 11 ± 3 to 7.3 ± 0.8 Å), as compared to that of the average NMR structure. [Nle^{15}]-HG[11−17]−βCD was docked to CCK$_2$-R(352−379) using the intermolecular NOEs as restraints. The backbone atoms in the putative TM domains were restrained to initial positions using a force constant of 200 kJ mol^{-1} nm^{-2}. The average backbone dihedral angles

[2] To simplify the description of the interaction in the ligand−receptor complex, the amino acids of the ligand will be denoted using the three-letter code and those of the receptor using the one-letter code.

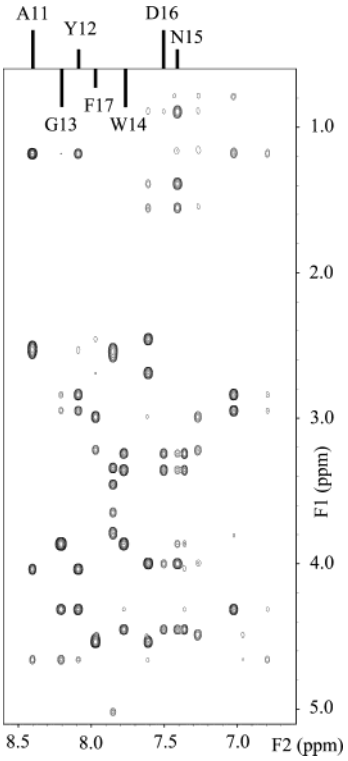

FIGURE 1: Expanded view of the amide−aliphatic region in the two-dimensional NOESY spectrum of [Nle[15]]-HG[11−17]−βCD (mixing time of 150 ms, 308 K).

of [Nle[15]]-HG[11−17]−βCD were restrained with a force constant of 500 kJ mol^{-1} rad^{-1} to the average values obtained during the NOE-restrained MD simulation of the ligand alone. The simulation was allowed to proceed for 200 ps at 300 K using the same conditions described above.

Models of the [Nle[15]]-HG[11−17]−βCD−CCK$_2$-R Complex. As described previously, the molecular model of the CCK$_2$-R was constructed by template forcing the backbone atoms in the putative TM domains of the CCK$_2$-R to those in the crystal structure of bovine rhodopsin (*29*). Extensive NOE-restrained MD simulations of the CCK-8−CCK$_2$-R complex, including two cycles of simulated annealing (50 ps at 1200−300 K), were used to generate a model of the ligand-binding pocket and to remove interhelical steric conflicts. After a stable structure for the CCK-8−CCK$_2$-R complex had been achieved (500 ps at 300 K), CCK-8 was replaced with [Nle[15]]-HG[11−17]−βCD. The ligand was manually docked using the intermolecular NOEs and binding orientations deduced from NOE-restrained MD simulations of the [Nle[15]]-HG[11−17]−βCD−CCK$_2$-R complex. NOE-restrained MD simulations of the [Nle[15]]-HG[11−17]−βCD−CCK$_2$-R complex were conducted for 200 ps at 300 K using the same conditions described above.

RESULTS

Structure of [Nle[15]]-HG[11−17]−βCD. The NOESY spectra of [Nle[15]]-HG[11−17]−βCD provided 89 unique and unambiguous NOEs (Figure 1). Of these, 21 were classified as sequential interresidue and 9 as nonsequential interresidue. Many of the structurally informative NOEs are summarized in Figure 2.

The NOE-derived distance restraints were used to generate an ensemble of 93 DG structures with distance violations of

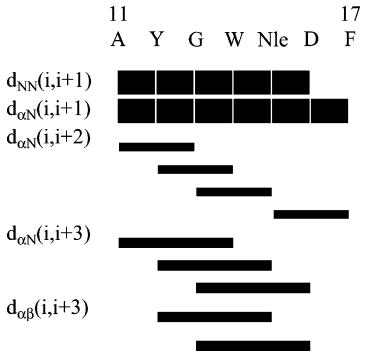

FIGURE 2: Summary of the structurally informative NOEs for [Nle[15]]-HG[11−17]−βCD observed from a NOESY spectrum collected at 308 K. The NOEs were classified as strong, medium, and weak according to the intensity of the integrated cross-peak volumes.

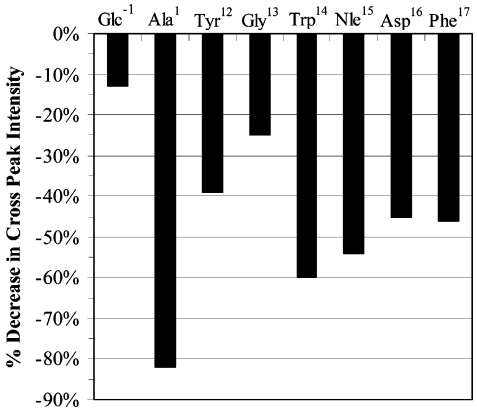

FIGURE 3: Radical-induced relaxation data of the ^{1}H resonances of [Nle[15]]-HG[11−17]−βCD following the addition of 0.5 mM 5-doxylstearate. The bars indicate the percent reduction in cross-peak intensity.

less than 0.3 Å and a backbone rmsd of 1.9 Å. The mean dihedral angles of Trp[14] ($\phi_{i+1} = -44° \pm 4°$ and $\psi_{i+1} = -44° \pm 6°$) and Nle[15] ($\phi_{i+1} = -99° \pm 9°$ and $\psi_{i+1} = 48° \pm 5°$) were consistent with a type I β turn between Gly[13] and Asp[16] ($\phi_{i+1} = -60°$, $\psi_{i+1} = -30°$, $\phi_{i+2} = -90°$, and $\psi_{i+2} = 0°$). The mean distances between the Cα and Cα(i,i+3), O and N(i,i+3), and O and HN(i,i+3) atoms were 6.1 ± 1.0, 3.6 ± 1.0, and 3.3 ± 1.0 Å, respectively. More than 70% of the generated DG structures satisfied the distance criteria for a hydrogen bond between the carbonyl oxygen of Gly[13] and the amide hydrogen of Asp[16]. The dihedral angles and aforementioned distances provide strong evidence of a type I β turn in the structure of [Nle[15]]-HG[11−17]−βCD.

The relative orientation of [Nle[15]]-HG[11−17]−βCD, with respect to the water−micelle interface, was determined by monitoring radical-induced relaxation of the backbone and side chain ^{1}H NMR signals. The cross-peak intensities of the amino acid residues were reduced 25−82%, while that of the first glucose monomer (Glc^{-1}) was reduced 13% (Figure 3). The relaxation data support a topological orientation in which the peptide is partially embedded in the hydrophobic phase of the micelle, with the β-cyclodextrin moiety closely associated with the water−micelle interface. Partial association of the βCD moiety with the water−micelle interface would not be unexpected, since the hydroxyl groups of βCD can form multiple stabilizing interactions with the zwitterionic headgroup of DPC.

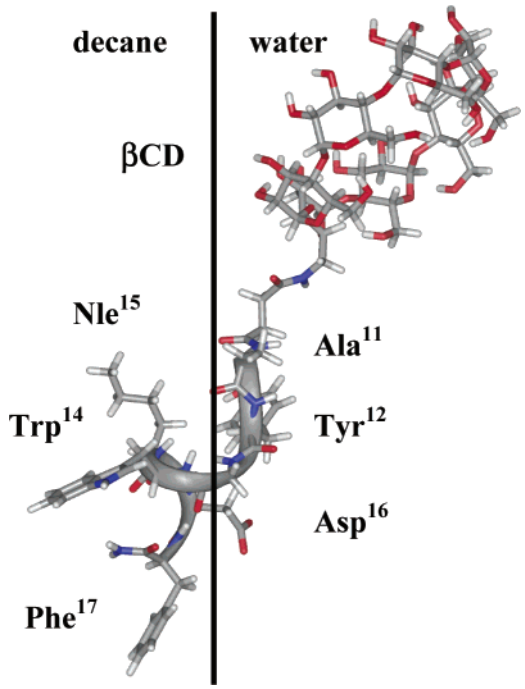

FIGURE 4: Structure of [Nle[15]]-HG[11−17]−βCD following 300 ps of an NOE-restrained MD simulation in a water/decane solvent box (300 K). The solvents have been removed for clarity. The line indicates the boundary between the phases.

The DG algorithm generated structures using a simplified force field composed of the distance, chiral volume, and van der Waals restraints without accounting for Coulombic and Lennard-Jones interactions, so a representative DG structure of [Nle[15]]-HG[11−17]−βCD was selected for further refinement by NOE-restrained MD in a membrane mimetic simulation cell composed of an immiscible layer of water and decane. The gastrin−βCD conjugate was positioned along the water−decane interface in accordance with the radical-induced relaxation data. The side chains of Ala[11], Trp[14], Nle[15], and Phe[17] were placed in the decane phase, while the remaining residues and the βCD moiety were projected into the aqueous phase. During the simulation, the hydrophobic side chains of the Trp[14], Nle[15], and Phe[17] residues became increasingly embedded in the decane phase (Figure 4). The Gly[13] and Asp[16] residues and the corresponding O−HN-(i,i+3) hydrogen bond were located along the water−decane interface, while the N-terminal residues and the βCD moiety resided in the aqueous phase. The mean backbone dihedral angles of [Nle[15]]-HG[11−17]−βCD extracted from the last 100 ps of the MD trajectory are provided in Table 1. Throughout the entire simulation, the backbone dihedral angles for Trp[14] and Nle[15] were consistent with a type I β turn.

Molecular Complex of [Nle[15]]-HG[11−17]−βCD with CCK$_2$-R(352−379). Addition of [Nle[15]]-HG[11−17]−βCD to CCK$_2$-R(352−379) produced a number of intermolecular NOEs and concentration-dependent chemical shift perturbations (Figure 5). Intermolecular NOEs were localized in the third extracellular loop region of the receptor domain between the amide of Ala[11] and Hα of S368, and between Hα of Tyr[12] and Asp[16] and Hε of R365. The most significant concentration-dependent chemical shift perturbations were observed for the amide resonances in the loop leading to the EC3 helix (G360 and G362), the EC3 helix (A363 and R365), and the TM7 (F374 and H376) regions of the receptor domain. Upon addition of the receptor domain, the intramolecular NOEs observed for the ligand remain the same, indicating no significant conformational change upon association with the receptor domain.

Table 1: Mean (±Standard Deviation) ϕ and ψ Dihedral Angles of [Nle[15]]-HG[11−17]−βCD Averaged over the Last 100 ps of an NOE-Restrained MD Simulation in a Water/Decane Simulation Cell (300 K)

	ϕ (deg)	ψ (deg)		ϕ (deg)	ψ (deg)
Ala[11]	64 ± 16	47 ± 34	Nle[15]	−77 ± 8	20 ± 11
Tyr[12]	−134 ± 6	75 ± 11	Asp[16]	−114 ± 16	−18 ± 16
Gly[13]	−105 ± 13	−80 ± 11	Phe[17]	177 ± 11	107 ± 28
Trp[14]	−46 ± 8	−48 ± 8			

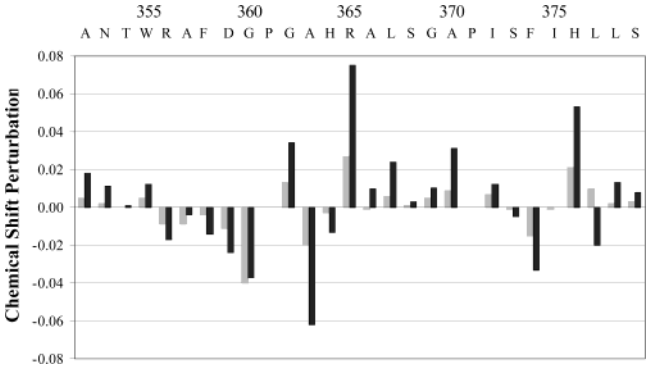

FIGURE 5: Amide ^{1}H chemical shift perturbations of the third extracellular loop of CCK$_2$, CCK$_2$-R(352−379), upon titration of [Nle[15]]-HG[11−17]−βCD. The black bars are for a 1:1 CCK$_2$-R-(352−379):[Nle[15]]-HG[11−17]−βCD ratio. For comparison, the chemical shift perturbations of the receptor domain upon addition of CCK-8 (using a ligand:receptor ratio of 0.6:1) are shown as gray bars.

The NMR analysis of the ligand−receptor complex is certainly hindered by overlap of the ^{1}H signals (both are natural abundance, synthetic products), and therefore, many intermolecular interactions may not be resolved and assigned. To identify additional intermolecular interactions that may contribute to the stability of the [Nle[15]]-HG[11−17]−βCD−CCK$_2$-R(352−379) complex, extensive NOE-restrained MD simulations, employing the unambiguously assigned NOEs, were carried out. The ligand was placed in the aqueous phase of the simulation cell in a variety of different starting orientations and 10 Å from the NOE-derived intermolecular contacts identified in the [Nle[15]]-HG-[11−17]−βCD−CCK$_2$-R(352−379) complex. During the MD simulations, the β turn of the ligand was oriented nearly perpendicular to the C-terminal end of the EC3 above TM7, with the C-terminal Phe[17] directed toward the putative TM bundle (Figure 6). The side chains of Trp[14], Nle[15], and Phe[17] were embedded in the decane phase in the vicinity of the hydrophobic strand leading from the central helix to TM7. The side chains of Tyr[12] and Asp[16] and the N-terminal β-cyclodextrin moiety were exposed to the aqueous phase of the simulation cell, while the side chain of Ala[11] was associated with the water−decane interface. The side chain of Nle[15] was located in a hydrophobic cusp formed by P371 and F374. Other notable van der Waals interactions (<3.6 Å) were identified between Ala[11] and

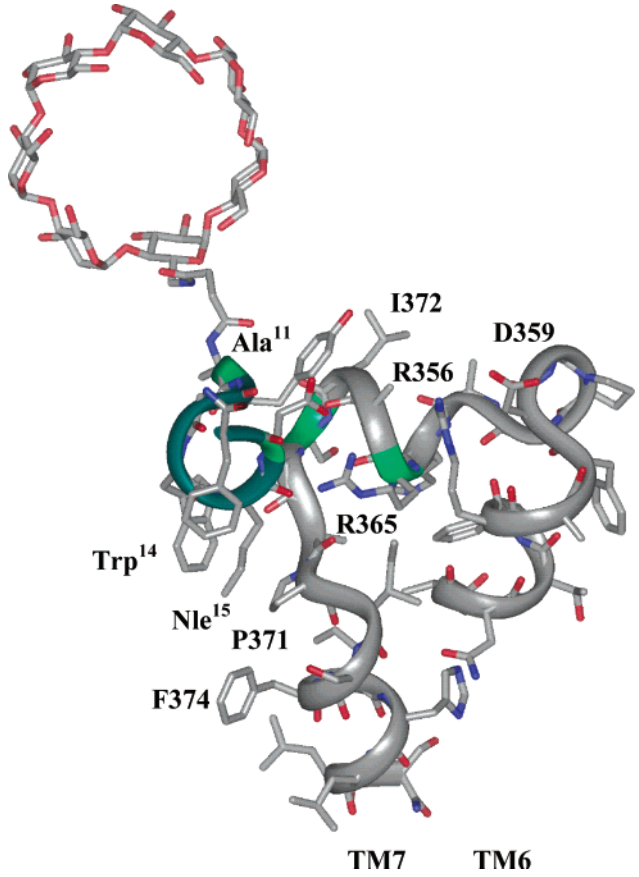

FIGURE 6: Complex of [Nle[15]]-HG[11−17]−βCD with CCK_2-R-(352−379) resulting from the NOE-restrained MD simulations. The ribbons of the ligand and receptor domain are colored dark green and gray, respectively. The ribbons of those residues forming intermolecular NOEs are colored light green.

G369, between Tyr[12] and R365, A366, L367, and G369, and between Trp[14] and G369 and P371. An electrostatic interaction was present between the carboxylate of Asp[16] and the guanidine of R365.

[Nle[15]]-HG[11−17]−βCD−CCK_2-R Complex. The topological orientation of [Nle[15]]-HG[11−17]−βCD in the molecular model of the ligand−receptor complex and the major binding interactions (≤3.6 Å) are depicted in Figure 7 and summarized in Table 2. Intermolecular interactions were identified in the upper third of TM1−3 and -7 and the EC1, EC2, and NT domains. The N- and C-termini of [Nle[15]]-HG[11−17]−βCD were located between TM1 and -7 and between TM2 and -3, respectively. As with CCK-8, the majority of the intermolecular interactions involved residues in the C-terminal tetrapeptide of [Nle[15]]-HG[11−17]−βCD (*29*). The side chain of Phe[17] was located in a well-defined hydrophobic pocket defined by residues in TM1 (L54, I58, and Y61), TM2 (I126 and V130), EC1 (I121 and F122), and EC2 (V206). The carboxamide formed stabilizing interactions with polar residues in EC2 (R201 and H207) and TM7 (H376). Electrostatic interactions were observed between the side chains of Asp[16] and R201 and R365. The side chains of Nle[15] and Trp[14] formed van der Waals interactions with TM1 (E53, R57, and L60) and TM7 (P371, I372, and S373). The amino-terminal residues and the βCD moiety were solvent-exposed and did not form appreciable interactions with the receptor.

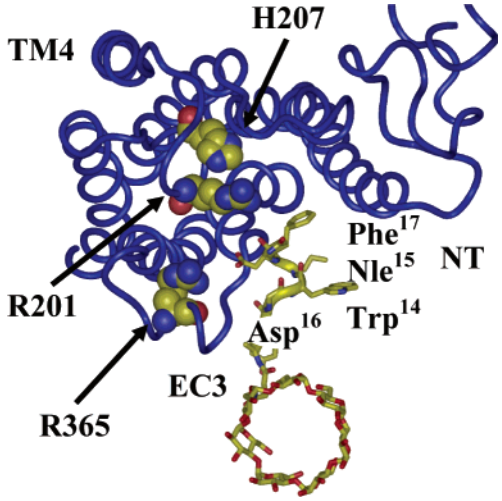

FIGURE 7: Extracellular face of the [Nle[15]]-HG[11−17]−βCD−CCK_2-R complex following 200 ps of NOE-restrained MD simulation (300 K) in a water/decane/water membrane mimetic simulation cell. The backbone atoms of the ligand and receptor are displayed as blue and black ribbons, respectively. The heavy atoms of the ligand are displayed as sticks, and the heavy atoms of R201, H207, and R365 in the receptor are displayed in CPK.

Table 2: Summary of Intermolecular Interactions in the [Nle[15]]-HG[11-17]−βCD−CCK_2-R Molecular Complex

residue	TM1/NT	TM2,3/EC1	TM4,5/EC2	TM6,7/EC3
NH_2		I121	R201, V206, H207	H376
Phe[17]	L54, R57, I58, Y61	N115, I121	R201, V206	I372
Asp[16]			R201	R365, A370, P371 I372
Nle[15]	R57, L60			G369, A370, P371 I372, S373
Trp[14]	E53, R57			P371
Gly[13]				P371
Tyr[12]				S368, G369, A370 P371, I372
Ala[11]				L367, S368, G369 A370

DISCUSSION

The conformational preferences of [Nle[15]]-HG[11−17]−βCD in DPC micelles contrast with the absence of structural order in aqueous solution (*19*), suggesting the turn structure is stabilized upon association with DPC micelles. The association of [Nle[15]]-HG[11−17]−βCD with DPC micelles is further supported by radical-induced relaxation of the ^{1}H NMR resonances. Perturbations in the phase transition temperature (T_c) of DMPC vesicles have been detected by differential scanning calorimetry upon addition of β-alanine-pentagastrin, CCK-9, DM-CCK-9, and DM-HG-17 (*7*, *20*, *43*−*45*). However, HG-17 had a negligible effect on the T_c, and results of CD studies of the aforementioned ligands in the presence of DMPC vesicles, as in aqueous solution, do not support ordered conformations (*7*, *10*). These apparently conflicting results may be attributed to differences in the lipid packing within DMPC vesicles and DPC micelles. The higher degree of order in the lipid packing of DMPC vesicles has been attributed to the expulsion of CCK-9 upon vesicle fusion, and has been proposed as a mechanism for neurotransmitter release in the synaptic junction (*7*).

The ordered conformations of [Nle^{15}]-HG[11−17]−βCD and HG-17 in DPC micelles and the relatively high binding affinity of DM-[Nle^{15}]-HG-17 provide evidence of a membrane-associated receptor recognition mechanism in the gastrin−CCK$_2$-R complex. Since the receptor initially recognizes the membrane-associated conformation of the ligand, the structural preferences observed in a membrane mimetic solvent system should resemble those of the bioactive conformation (*5*). A comparison of the structural features of an analogue of pituitary adenylate cyclase activating peptide in DPC micelles and while bound to its GPCR revealed only minor differences in conformation, providing further evidence of the membrane-bound pathway and the use of DPC as a membrane mimetic (*46*).

The conformational features in the C-terminus of [Nle^{15}]-HG[11−17]−βCD were similar to those previously reported for CCK-8 and CCK-15 in the same solvent system. Superposition of the backbone atoms of the C-terminal hexapeptide taken from the average coordinates of [Nle^{15}]-HG[11−17]−βCD and CCK-8 during the last 100 ps of NOE-restrained MD simulations produced an rmsd of 1.8 Å (*12*, *13*). The extremely hydrophilic and bulky N-terminal moiety of [Nle^{15}]-HG[11−17]−βCD did not appear to influence the structure of the peptide. The observation of a β turn in analogues of gastrin and CCK suggests a C-terminal turn structure is a necessary prerequisite for high-affinity binding of the ligand to the CCK$_1$-R and CCK$_2$-R (*12*, *13*, *28*, *29*).

The NOE-derived contacts in the [Nle^{15}]-HG[11−17]−βCD−CCK$_2$-R(352−379) complex resulted in a ligand binding mode that was also capable of simultaneously satisfying the NOE-derived contacts in the CCK-8−CCK$_2$-R(352−379) complex (*29*). The similarity in the chemical shift perturbation profiles and the proximity of the intermolecular NOEs suggest the two ligands bind to CCK$_2$-R(352−379) in a similar manner. Given the large, bulky βCD moiety, this observation clearly indicates the N-terminus of the ligand is removed from the tight steric constraints of the receptor as we had surmised previously with CCK-8 (*29*).

The proposed ligand binding mode for [Nle^{15}]-HG[11−17]−βCD in the NOE-restrained model of the [Nle^{15}]-HG-[11−17]−βCD−CCK$_2$-R complex places the C-terminus in the upper third of the TM bundle in the proximity of TM2 and -3. The ligand binding mode is stabilized by Coulombic interactions between Asp^{16} and R201 and R365. The topological orientation and binding interactions in the NOE-restrained molecular model of the [Nle^{15}]-HG[11−17]−βCD−CCK$_2$-R complex were nearly identical to those in the CCK-8−CCK$_2$-R complex (*29*). A number of key residues in the ligand-binding pocket of the [Nle^{15}]-HG[11−17]−βCD−CCK$_2$-R complex were previously identified by receptor chimera and site-directed mutagenesis. Replacement of restriction endonuclease-defined segments in the CCK$_2$-R with the corresponding residues in the CCK$_1$-R revealed a segment of six amino acids (Q^{204}CVHRW^{209}) in the EC2 domain of the CCK$_2$-R that could account for the selective loss of HG-17 binding affinity (*47*). Subsequent site-directed mutagenesis studies with the CCK-8−CCK$_2$-R complex implicated the C-terminal Asp^{32} residue of CCK-8 and H207 in high-affinity ligand binding (*16*). In the NOE-restrained molecular models of the [Nle^{15}]-HG[11−17]−βCD and CCK-8−CCK$_2$-R complexes, stabilizing interactions were observed between R201 and H207, suggesting the reduced affinity for the H207 mutant may be attributed to indirect effects rather than direct interactions between the C-terminal Asp and H207. However, the proximity of R201 and H207 in the NOE-restrained molecular model of the CCK$_2$-R complex does not rule out a direct interaction between Asp^{16} and H207. The proposed ligand binding mode is further supported by a single-point mutation in the extracellular portion of TM7, H376L, which resulted in a 17-fold reduction in the binding affinity of HG-17 (*48*). Intermolecular interactions between H376 and the carboxamide of [Nle^{15}]-HG[11−17]−βCD were observed in the NOE-restrained molecular model of the ligand−receptor complex, confirming the importance of this residue.

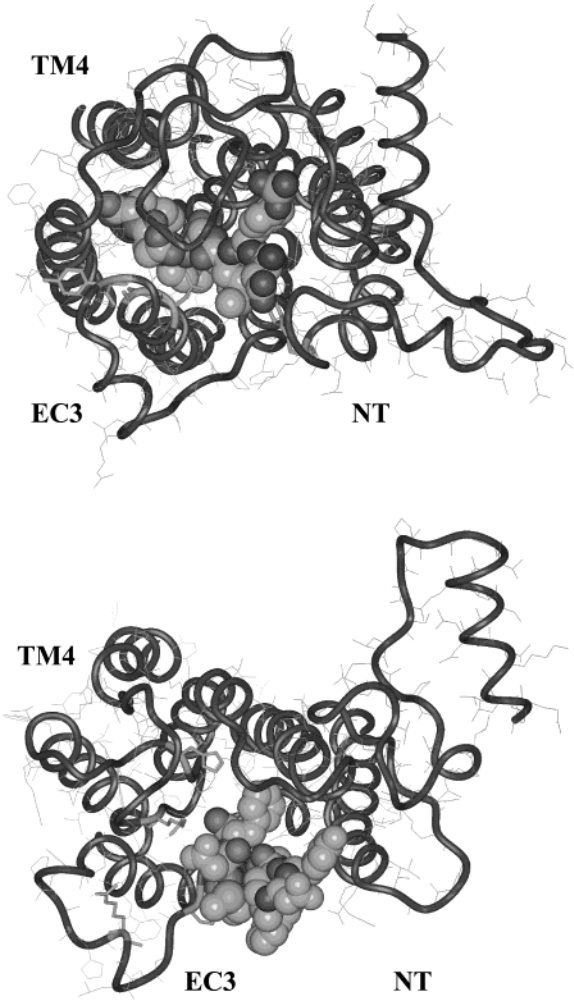

FIGURE 8: Comparison of the CCK-8 binding modes in molecular models of the CCK$_1$-R (top) and CCK$_2$-R (bottom) complexes following 700 ps of NOE-restrained MD simulation (300 K) in a water/decane/water solvent box, as viewed from the extracellular face of the receptor. The backbone of the receptors and the heavy atoms of CCK-8 are displayed as a ribbon and in CPK colors, respectively.

The NOE-restrained molecular models of the [Nle^{15}]-HG-[11−17]−βCD and CCK-8−CCK$_2$-R complexes produced a distinct ligand binding mode, as compared to the NOE-retrained molecular model of the CCK-8−CCK$_1$-R complex (Figure 8) (*28*, *29*). The putative peptide ligand-binding site in the CCK$_2$-R is composed of a shallow hydrophobic pocket near the confluence of TM2 and -3, while the CCK$_1$-R is composed of a much deeper hydrophobic pocket near the

confluence of TM3−5. The proposed differences in the location and extent of TM bundle penetration are supported by the subtype selectivity of cholecystokinin and gastrin analogues. High-affinity ligand binding in the CCK_1-R requires the carboxyamidated C-terminal heptapeptide of CCK sulfated at Tyr^{27}, whereas for the CCK_2-R, only the carboxyamidated C-terminal tetrapeptide is necessary. The high binding affinity of [Nle^{15}]-HG[14−17]−βCD, the tetrapeptide analogue of [Nle^{15}]-HG[11−17]−βCD, provides further evidence of a shallow ligand-binding pocket in the CCK_2-R (*19*). The postulated turn structure in tetragastrin and the steric bulk associated with the β-cyclodextrin moiety would prevent significant TM bundle penetration, without resulting in a significant alteration in the conformations of the extracellular domains and a concomitant reduction in ligand binding affinity.

In summary, the structural order of [Nle^{15}]-HG[11−17]−βCD in the presence of a membrane mimetic solvent system and the radical-induced relaxation of the ^{1}H NMR resonances support a membrane-associated receptor recognition mechanism. The ligand binding mode and intermolecular interactions deduced in the NOE-restrained MD molecular models of the [Nle^{15}]-HG[11−17]−βCD and CCK-8−CCK_2-R complexes are in good agreement and provide new insight into the role of electrostatic interactions in the ligand-binding pocket.

REFERENCES

1. Rehfeld, J. F., and van Solinge, W. W. (1994) The tumor biology of gastrin and cholecystokinin, *Adv. Cancer Res. 63*, 295−347.
2. Wank, S. A. (1998) G protein-coupled receptors in gastrointestinal physiology. I. CCK receptors: an exemplary family, *Am. J. Physiol. 274*, G607−G613.
3. Wank, S. A. (1995) Cholecystokinin receptors, *Am. J. Physiol. 269*, G628−G646.
4. Noble, F., Wank, S. A., Crawley, J. N., Bradwejn, J., Seroogy, K. B., Hamon, M., and Roques, B. P. (1999) International Union of Pharmacology. XXI. Structure, distribution, and functions of cholecystokinin receptors, *Pharmacol. Rev. 51*, 745−781.
5. Pellegrini, M., and Mierke, D. F. (1999) Structural Characterization of Peptide Hormone/Receptor Interactions by NMR Spectroscopy, *J. Pept. Sci. 51*, 208−220.
6. Albrizio, S., Carotenuto, A., Fattorusso, C., Moroder, L., Picone, D., Temussi, P. A., and D'Ursi, A. (2002) Environmental mimic of receptor interaction: conformational analysis of CCK-15 in solution, *J. Med. Chem. 45*, 762−769.
7. Moroder, L., and Lutz, J. (1996) Potential bioactive conformations of hormones of the gastrin family, *Stud. Nat. Prod. Chem. 18*, 819−869.
8. Mammi, S., and Peggion, E. (1990) Conformational studies of human [15-2-aminohexanoic acid]little gastrin in sodium dodecyl sulfate micelles by ^{1}H NMR, *Biochemistry 29*, 5265−5269.
9. Mammi, S., Foffani, M. T., Peggion, E., Galleyrand, J. C., Bali, J. P., Simonetti, M., Gohring, W., Moroder, L., and Wunsch, E. (1989) Conformational and biological properties of the Ala10 analogue of human des-Trp1,Nle12-minigastrin, *Biochemistry 28*, 7182−7188.
10. Peggion, E., Foffani, M. T., Wunsch, E., Moroder, L., Borin, G., Goodman, M., and Mammi, S. (1985) Conformational properties of gastrin fragments of increasing chain length, *Biopolymers 24*, 647−666.
11. Peggion, E., Jaeger, E., Knof, S., Moroder, L., and Wuensch, E. (1981) Conformational aspects of gastrin-related peptides: a circular dichroism study, *Biopolymers 20*, 633−652.
12. Pellegrini, M., and Mierke, D. F. (1999) The molecular complex of cholecystokinin-8 and N-terminus of the cholecystokinin A receptor by NMR spectroscopy, *Biochemistry 38*, 14775−14783.
13. Giragossian, C., Stone, S., Papini, A. M., Moroder, L., and Mierke, D. F. (2002) Conformational and molecular modeling studies of sulfated cholecystokinin-15, *Biochem. Biophys. Res. Commun. 293*, 1053−1059.
14. Anders, J., Bluggel, M., Meyer, H. E., Kuhne, R., ter Laak, A. M., Kojro, E., and Fahrenholz, F. (1999) Direct identification of the agonist binding site in the human brain CholecystokininB receptor, *Biochemistry 38*, 6043−6055.
15. Gigoux, V., Maigret, B., Escrieut, C., Silvente-Poirot, S., Bouisson, M., Fehrentz, J. A., Moroder, L., Gully, D., Martinez, J., Vaysse, N., and Fourmy, A. D. (1999) Arginine 197 of the cholecystokinin-A receptor binding site interacts with the sulfate of the peptide agonist cholecystokinin, *Protein Sci. 8*, 2347−2354.
16. Silvente-Poirot, S., Escrieut, C., Gales, C., Fehrentz, J. A., Escherich, A., Wank, S. A., Martinez, J., Moroder, L., Maigret, B., Bouisson, M., Vaysse, N., and Fourmy, D. (1999) Evidence for a direct interaction between the penultimate aspartic acid of cholecystokinin and histidine 207, located in the second extracellular loop of the cholecystokinin B receptor, *J. Biol. Chem. 274*, 23191−23197.
17. Lutz, J., Romano-Gotsch, R., Escrieut, C., Fourmy, D., Matha, B., Muller, G., Kessler, H., and Moroder, L. (1997) Mapping of ligand binding sites of the cholecystokinin-B/gastrin receptor with lipo-gastrin peptides and molecular modeling, *Biopolymers 41*, 799−817.
18. Moroder, L. (1997) On the mechanism of hormone recognition and binding by the CCK-B/gastrin receptor, *J. Pept. Sci. 3*, 1−14.
19. Schaschke, N., Fiori, S., Weyher, E., Escrieut, C., Fourmy, D., Muller, G., and Moroder, L. (1998) Cyclodextrin as Carrier of Peptide Hormones. Conformational and Biological Properties of β-Cyclodextrin/Gastrin Constructs, *J. Am. Chem. Soc. 120*, 7030−7038.
20. Moroder, L., Romano, R., Guba, W., Mierke, D. F., Kessler, H., Delporte, C., Winand, J., and Christophe, J. (1993) New evidence for a membrane-bound pathway in hormone receptor binding, *Biochemistry 32*, 13551−13559.
21. Schwyzer, R. (1995) In search of the 'bio-active conformation': is it induced by the target cell membrane? *J. Mol. Recognit. 8*, 3−8.
22. Schwyzer, R. (1992) How do peptides interact with lipid membranes and how does this affect their biological activity, *Braz. J. Med. Biol. Res. 25*, 1077−1089.
23. Schwyzer, R. (1991) Peptide−membrane interactions and a new principle in quantitative structure−activity relationships, *Biopolymers 31*, 785−792.
24. Kunishima, N., Shimada, Y., Tsuji, Y., Sato, T., Yamamoto, M., Kumasaka, T., Nakanishi, S., Jingami, H., and Morikawa, K. (2000) Structural basis of glutamate recognition by a dimeric metabotropic glutamate receptor, *Nature 407*, 971−977.
25. West, A. P., Jr., Llamas, L. L., Snow, P. M., Benzer, S., and Bjorkman, P. J. (2001) Crystal structure of the ectodomain of Methuselah, a *Drosophila* G protein-coupled receptor associated with extended lifespan, *Proc. Natl. Acad. Sci. U.S.A. 98*, 3744−3749.
26. Yeagle, P. L., and Albert, A. D. (2002) Use of nuclear magnetic resonance to study the three-dimensional structure of rhodopsin, *Methods Enzymol. 343*, 223−231.
27. Mierke, D. F., and Giragossian, C. (2001) Peptide hormone binding to G-protein-coupled receptors: structural characterization via NMR techniques, *Med. Res. Rev. 21*, 450−471.
28. Giragossian, C., and Mierke, D. F. (2001) Intermolecular interactions between cholecystokinin-8 and the third extracellular loop of the cholecystokinin A receptor, *Biochemistry 40*, 3804−3809.
29. Giragossian, C., and Mierke, D. F. (2002) Intermolecular interactions between cholecystokinin-8 and the third extracellular loop of the cholecystokinin-2 receptor, *Biochemistry 41*, 4560−4566.
30. Giragossian, C., Sugg, E. E., Szewczyk, J. R., and Mierke, D. F. (2003) Intermolecular interactions between peptidic and nonpeptidic agonists and the third extracellular loop of the cholecystokinin 1 receptor, *J. Med. Chem. 46*, 3476−3482.
31. States, D. J., Haberkorn, R. A., and Ruben, D. J. (1982) A Two-Dimensional Nuclear Overhauser Experiment with Pure Absorption Phase in Four Quadrants, *J. Magn. Reson. 48*, 286−292.
32. Braunschweiler, L., and Ernst, R. R. (1983) Coherence Transfer by Isotropic Mixing: Application to Proton Correlation Spectroscopy, *J. Magn. Reson. 53*, 521−528.
33. Bax, A., and Davis, D. G. (1985) MLEV-17 Based Two-Dimensional Homonuclear Magnetization Transfer Spectroscopy, *J. Magn. Reson. 65*, 355−360.

34. Macura, S., Huang, Y., Suter, D., and Ernst, R. R. (1981) Two-Dimensional Chemical Exchange and Cross-Relaxation Spectroscopy of Coupled Nuclear Spins, *J. Magn. Reson. 43*, 259−281.
35. Jeener, J., Meier, B. H., Bachmann, P., and Ernst, R. R. (1979) Investigation of Exchange Processes by Two-Dimensional NMR Spectroscopy, *J. Chem. Phys. 71*, 4546−4553.
36. Piotto, M., Saudek, V., and Sklenar, V. (1992) Gradient-tailored excitation for single-quantum NMR spectroscopy of aqueous solutions, *J. Biomol. NMR 2*, 661−665.
37. Delaglio, F., Grzesiek, S., Vuister, G. W., Zhu, G., Pfeifer, J., and Bax, A. (1995) NMRPipe: a multidimensional spectral processing system based on UNIX pipes, *J. Biomol. NMR 6*, 277−293.
38. Goddard, T. D., and Kneller, D. G. (2001) Sparky 3.0, University of California, San Francisco.
39. Wuthrich, K., Billeter, M., and Braun, W. (1983) Pseudo-Structures for the 20 Common Amino Acids for Use in Studies of Protein Conformations by Measurements of Intramolecular Proton−Proton Distance Constraints with Nuclear Magnetic Resonance, *J. Mol. Biol. 169*, 949−961.
40. Brown, L. R., Bosch, C., and Wuthrich, K. (1981) Location and orientation relative to the micelle surface for glucagon in mixed micelles with dodecylphosphocholine: EPR and NMR studies, *Biochim. Biophys. Acta 642*, 296−312.
41. Havel, T. F. (1991) An evaluation of computational strategies for use in the determination of protein structure from distance geometry constraints obtained by nuclear magnetic resonance, *Prog. Biophys. Mol. Biol. 56*, 43−78.
42. Palczewski, K., Kumasaka, T., Hori, T., Behnke, C. A., Motoshima, H., Fox, B. A., Le Trong, I., Teller, D. C., Okada, T., Stenkamp, R. E., Yamamoto, M., and Miyano, M. (2000) Crystal structure of rhodopsin: A G protein-coupled receptor, *Science 289*, 739−745.
43. Romano, R., Bayerl, T. M., and Moroder, L. (1993) Lipophilic derivatization and its effect on the interaction of cholecystokinin (CCK) nonapeptide with phospholipids, *Biochim. Biophys. Acta 1151*, 111−119.
44. Romano, R., Dufresne, M., Prost, M. C., Bali, J. P., Bayerl, T. M., and Moroder, L. (1993) Peptide hormone-membrane interactions. Intervesicular transfer of lipophilic gastrin derivatives to artificial membranes and their bioactivities, *Biochim. Biophys. Acta 1145*, 235−242.
45. Surewicz, W., and Epand, R. M. (1985) Role of peptide structure in lipid-peptide interactions: high-sensitivity differential scanning calorimetry and electron spin resonance studies of the structural properties of dimyristoylphosphatidylcholine membranes interacting with pentagastrin-related pentapeptides, *Biochemistry 24*, 3135−3144.
46. Inooka, H., Ohtaki, T., Kitahara, O., Ikegami, T., Endo, S., Kitada, C., Ogi, K., Onda, H., Fujino, M., and Shirakawa, M. (2001) Conformation of a peptide ligand bound to its G-protein coupled receptor, *Nat. Struct. Biol. 8*, 161−165.
47. Silvente-Poirot, S., and Wank, S. A. (1996) A segment of five amino acids in the second extracellular loop of the cholecystokinin-B receptor is essential for selectivity of the peptide agonist gastrin, *J. Biol. Chem. 271*, 14698−14706.
48. Kopin, A. S., McBride, E. W., Quinn, S. M., Kolakowski, L. F., Jr., and Beinborn, M. (1995) The role of the cholecystokinin-B/gastrin receptor transmembrane domains in determining affinity for subtype-selective ligands, *J. Biol. Chem. 270*, 5019−5023.

BI035509W